NASA Electronic Parts and Packaging (NEPP) Program

NEPP Task: Reliability of Advanced Wet and Solid Tantalum Capacitors

Deformation of Cases in High Capacitance Value Wet Tantalum Capacitors under Environmental Stresses

Alexander Teverovsky

ASRC Federal Space and Defense
Alexander.A.Teverovsky@nasa.gov

Worked performed at NASA Goddard Space Flight Center

2016

Deliverable to NASA Electronic Parts and Packaging (NEPP) Program to be published on nepp.nasa.gov.

Deformation of Cases in High Capacitance Value Wet Tantalum Capacitors under Environmental Stresses

Abstract

Internal gas pressure in hermetic wet tantalum capacitors is created by air, electrolyte vapor, and gas generated by electrochemical reactions at the electrodes. This pressure increases substantially with temperature and time of operation due to excessive leakage currents. Deformation of the case occurs when the internal pressure exceeds pressure of the environments and can raise significantly when a part operates in space. Contrary to the cylinder case wet tantalum capacitors that have external sealing by welding and internal sealing provided by the Teflon bushing and crimping of the case, no reliable internal sealing exists in the button case capacitors. Single seal design capacitors are used for high capacitance value wet tantalum capacitors manufactured per DLA L&M drawings #04003, 04005, and 10011, and require additional analysis to assure their reliable application in space systems. In this work, leakage currents and case deformation of button case capacitors were measured during different environmental test conditions. Recommendations for derating, screening and qualification testing are given. This work is a continuation of a series of NEPP reports related to quality and reliability of wet tantalum capacitors [1-4]

Background

Case deformation in wet tantalum capacitors is due to the difference between the internal pressure of gases and vapors inside the case and external environmental pressure. Excessive internal pressure might be due to gas generation as a result of electrochemical reactions at the electrodes or to the pressure of electrolyte vapor that increases substantially with temperature during operation or storage conditions [3]. Hydrogen, that is the major constituent of gases generated during operation, can cause embrittlement of tantalum and enhance case rupture resulting in catastrophic failures of the part. Another mechanism of failure is due to penetration of the electrolyte to the glass seal area that might cause excessive leakage currents, corrosion of the tubing weld, and hermeticity loss.

Due to the absence of external pressure in vacuum, case deformation and risks of failures increase when a part operates in space. For this reason, additional analysis is necessary to determine adequate quality assurance measures for the button case capacitors intended for space applications.

High capacitance value wet tantalum capacitors are used in space applications as energy storage devices that allow a fast charge delivery in a variety of power supply systems. These parts are manufactured to DLA LAM drawings #04003, #04004, #04005, and #10011 (commercial equivalents are THQ series from Evans and HE series from Vishay). To increase volumetric efficiency compared to traditional, cylinder case wet tantalum capacitors that are manufactured per MIL-PRF-39006, these parts employ a button-case design as shown in Fig.1. Contrary to the military grade capacitors that are manufactured with internal sealing provided by Teflon bushing and crimping of the case, first THQ designs of capacitors did not have protection of the glass seal area, and their hermeticity was provided only by welding of the lid and tubing.

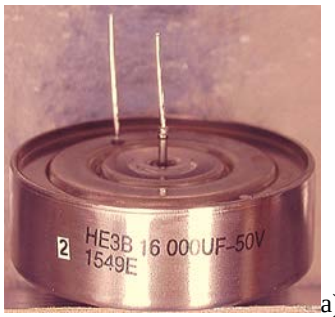

a)


b)

Figure 1. Examples of button-case designs of wet tantalum capacitors: THQ series (DWG#04005) from Evans (a) and HE series (DWG#10011) from Vishay.

First THQ-style capacitors were manufactured before 1996. The parts were assembled dry, with electrolyte added through a small hole in the cover that was closed by a welded tantalum plug [5]. A schematic and internal features of THQA capacitors manufactured in 2004 and 2013 are shown in Fig.2. Testing of THQA capacitors manufactured in 2004 showed that these parts often fail hermeticity during various environmental tests. For this reason, in later versions of this design, Teflon or rubber washers were installed to protect the glass seal area. Note that all HE3 capacitors have internal rubber seals.

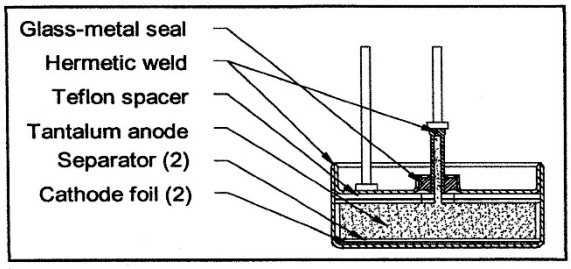

a)
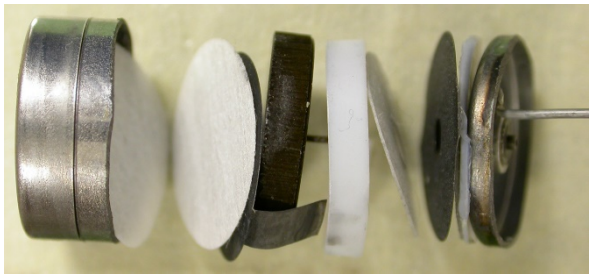
b)
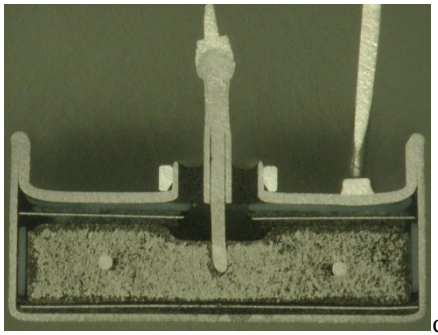
c)
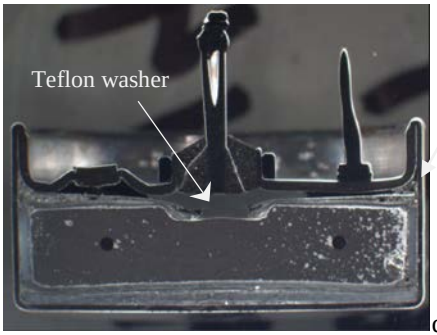

d)
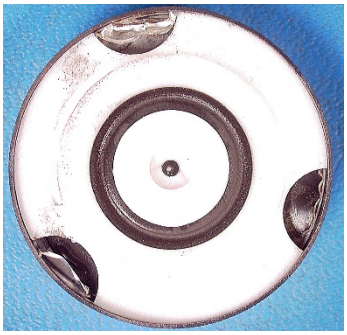
e)

Figure 2. A schematic (a) and internal elements (b – d) of THQA and HE3 (e) capacitors. (b) Internal components of the disassembled THQA capacitor. Cross-sectioning of THQA capacitors manufactured in 2004 (c) and in 2008 (d). Contrary to 2004 design (c), capacitors manufactured in 2008 (d) had a Teflon washer protecting the glass seal area. Note that capacitors manufactured in 2013 had rubber instead of Teflon washers. Fig.(e) shows a top view of HE3 capacitor after lid removal. Note a rubber seal in the groove of the Teflon separator.

Fig.3 shows variations in the mass of 240 μF 125 V DWG#04005 capacitors manufactured in 2004, weighed after 200 hours of room temperature testing at rated voltage and then during high temperature storage at 175 ºC after 65 hr, 165 hr, and 320 hr. Approximately half of the parts (17 samples total were tested) had noticeable (up to 80 mg) decreases in the mass caused by the electrolyte leak. However, no catastrophic failures during these tests was observed. In all cases the leak was in the tubing weld area (see Fig 3c).

Analysis shows that temperature increase from room to 175 ºC increases electrolyte leak more than two orders of magnitude [3], so a part having the measured leak rate 10^{-8} atm*cc/s should have lost less than 10 mg of electrolyte during two weeks of storage at 175 ºC. Considering that initially, based on the fine leak testing, the parts were hermetic, it is possible that the leak was caused by corrosion of tantalum in the weld area. It is known that pure tantalum is immune to attack by sulfuric acid at temperatures below ~ 200 ºC. However, in the presence of contaminations, and specifically, carbon, the weld area can be attacked by acids. It is also possible that the seal was compromised by excessive internal pressure and deformation of the case.

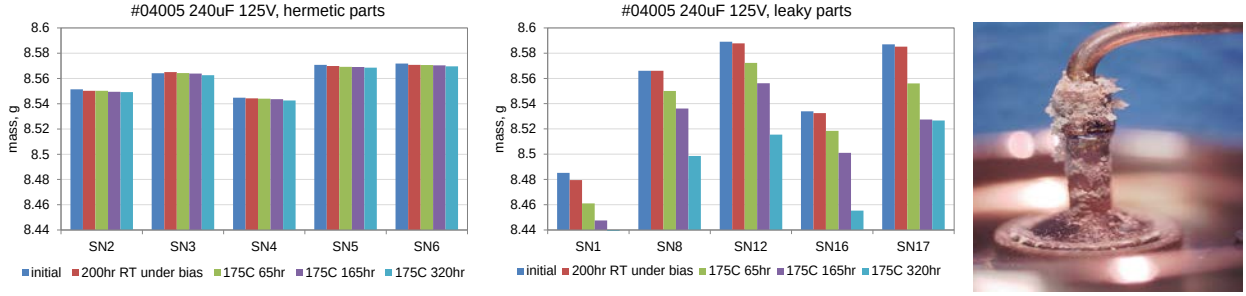

a) b) c)

Figure 3. Variation of mass of DWG#04005 capacitors manufactured in 2004 during environmental testing. (a) hermetic parts; (b) leaky parts; (c) remnants of electrolyte on a tubing in a leaky part after the testing.

To assure proper welding of tantalum, oxygen and other oxidative agents should be excluded from the weld area. This is difficult to achieve during welding of the tube in a capacitor with electrolyte. To improve hermeticity and avoid leak failures under environmental stresses, currently manufacturers are employing additional sealing of the outlet area. For this purpose, washers are squeezed between the anode slugs/separator and outlets by applying pressure to the lid before sealing. This is supposed to protect the glass area and prevent electrolyte from getting to the tubing. However, the effectiveness of this protection is difficult to verify and control. Increasing internal gas pressure during operation of the parts or exposure to high temperatures will cause case lid deformation and reduce the pressure to the washer thus allowing permeation of electrolyte to the glass seal area.

The purpose of this work was analysis of case deformations with temperature and electrical stresses for button-case capacitors. Experiments were carried out using 16 mF 50 V HE3B163M050BZSS capacitors (DLA DWG#10011), and 12 mF 63 V THQ3063123 capacitors (DLA DWG#04003). First, performance of the parts was characterized over a wide range of voltages and temperatures, and then deformation of the case was studied under different types of stresses using a laser-optical displacement measuring system. To accelerate degradation of the parts and evaluate behavior of the parts when the internal protection of the glass seal is compromised, the parts were stressed at conditions exceeding the specified maximum operating temperature (125 ºC) and voltage (2/3VR) for these capacitors.

Performance of HE3 16 mF 50V and THQ3 12 mF 63V capacitors

Leakage currents specified for HE3 capacitors are increasing linearly with the value of capacitance as it is shown in Fig.4a. Some deviation from the linearity exists for capacitors rated to 25 V. The linearity remains valid when maximum leakage currents are plotted against CV values as shown in Fig. 4b. Note, that contrary to a simple rule that determins DCL values for chip tantalum capacitors (DCL = 0.01×CV for MnO2 and DCL = 0.1×CV for polymer capacitors), no simple relationship exists for wet tantalum capacitors. For these parts, the limit is most likely set by a combination of statistical analysis, internal manufacturers' rules, and marketing. Comparison of DCL requirements for HE3 and THQ3 capacitors (see Fig. 4b) shows that similar parts from different manufacturers have same requirements. This confirms an important role of marketing in setting DCL limits for commercial and DLA drawing products.

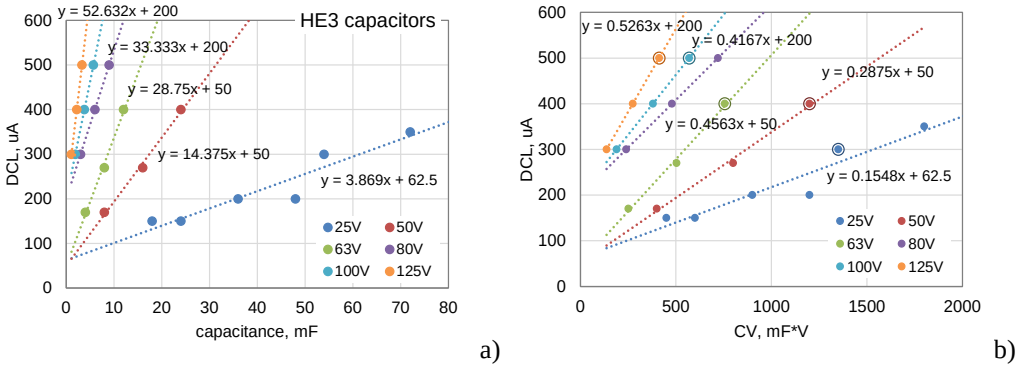

a) b)

Figure 4. Variations of the maximum specified leakage currents with capacitance (a) and CV values (b). Solid marks correspond to HE3 and circles to THQ3 capacitors. Not that circles coinside with the marks in all cases.

Variations of leakage currents with time at room temperature and 85 ºC are shown in Fig. 5. Results at room temperature show reproducible and stable leakage currents for HE3 and a relatively large spread for THQ3 capacitors. Two out of six THQ samples had unstable leakage currents after 100 hours of testing. For high-value capacitors intrinsic currents prevail over absorption currents after ~ 1000 sec.

Leakage currents in HE3 capacitors measured after 5 min of electrification were within the range from 40 μA to 60 μA, which is several times below the specified value of 270 μA. Measurements at 85 ºC during 340 hours showed that currents are decreasing with time, and although some instability was observed, the currents remain close for different parts in the group. Currents measured at 85 ºC were approximately an order of magnitude greater than at room temperature, from 400 μA to 500 μA. However, for these parts currents at 85 ºC are not specified, which limits the capabilities of the quality assurance system.

For THQ3 capacitors, leakage currents at room temperature were in the range from 60 μA to 150 μA, which is below the limit of 400 μA. At 85 ºC the currents increased up to 800 μA. For both part types currents decreased gradually with time under bias during hundreds of hours of testing at room temperature and 85 ºC.

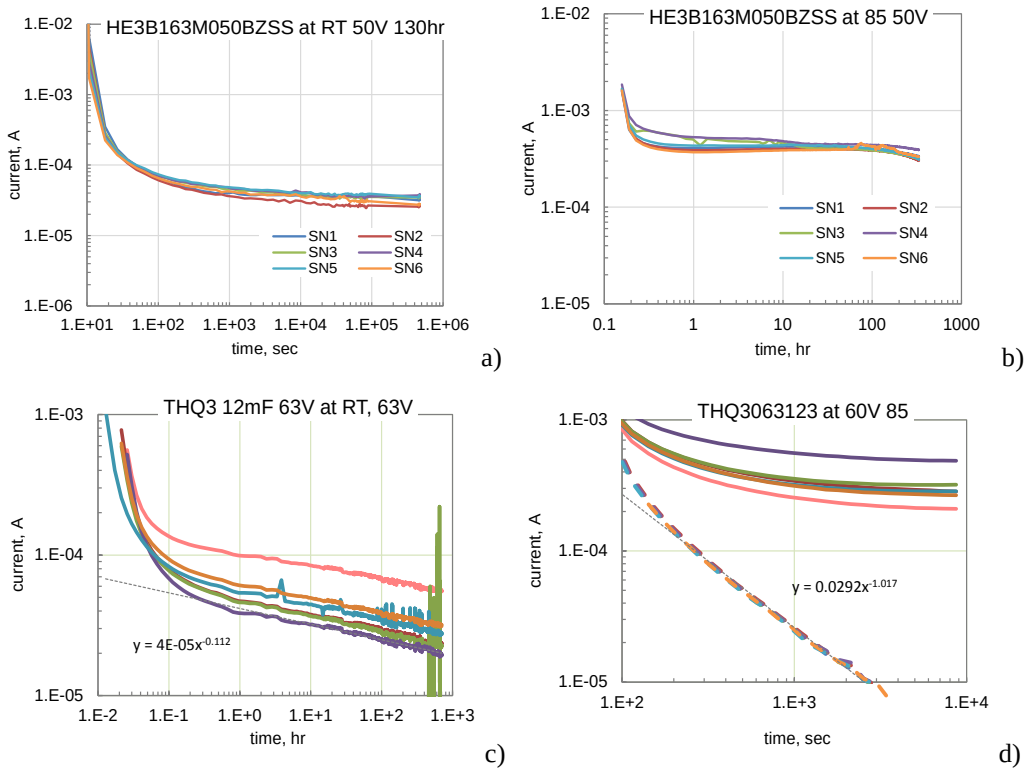

Figure 5. Variations of currents with time at room temperature (a, c) and 85 ºC (b, d) for HE3 (a, b) and THQ3 (c, d) capacitors. Dashed lines in Fig. (d) indicate depolarization (absorption) currents.

Relaxation of currents at different temperatures and voltages for THQ3 capacitors are shown in Fig. 6. At 50 V absorption currents prevail at room temperature (RT) for at least one hour of electrofication (see Fig. 6a). Increasing temperature to 85 ºC makes intrinsic currents evident after ~ 0.5 hour and after a few minutes at 125 ºC. Contrary to intrinsic currents that increase from RT to 125 ºC by more than 2 orders of magnitude, absorption or depolarization currents are increasing less than 2 times (see Fig. 6b). At 85 ºC and 10 V, polarization and dapolarization currents are similar (see Fig. 6c), but the prevelance of intrinsic currents became obvious as the voltage increases to 25 V and 50 V. Based on measurements of leakage currents at 50 V the activation energy of intrinsic leakage currents is ~0.65 eV (Fig. 6d).

To present *I-V* characteristics of the part in Schottky coordinates, *ln(I)* vs. $E^{0.5}$, the thickness of the dielectric was calculated as $d = 1.8*VR*\alpha_F$, where *d* is in nm, VR=63 V is the rated voltage, and α_F, which is the voltage formation coefficient, was assumed to be 2. Calculations yielded *d* = 227 nm. Results in Fig. 6e show that the slope of *ln(I)* vs. $E^{0.5}$ characteristics is ~6E-4 $(m/V)^{0.5}$, which is close to the theoretical value for the Schottky model, 6.5E-4 $(m/V)^{0.5}$ [3], and indicate that the currents are limited by a barrier at the electrolyte/Ta2O5 interface.

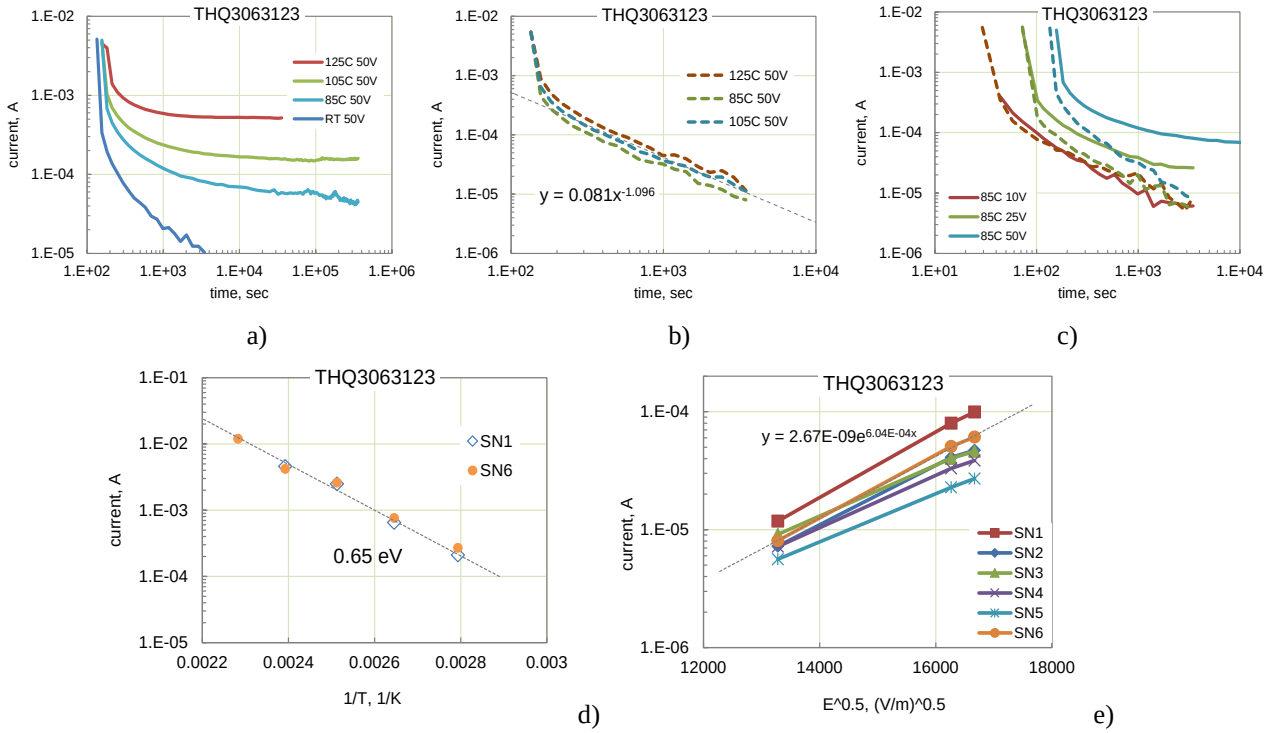

Figure 6. Leakage currents in THQ capacitors. (a – c) Relaxation of leakage currents at different temperatures and voltages; (d) temperature dependence of leakage currents in Arrhenius coordinates; (e) current-electric field characteristics in Schottky coordinates.

Variations of polarization and depolarization currents with time at temperatures from -55 ºC to +85 ºC for SNs 1 to 3 of HE3 capacitors are shown in Fig.7. At low temperatures, -55 ºC, polarization and depolarization currents are similar. At room temperature (RT) and rated voltage, intrinsic currents are several times greater than absorption currents after 1000 sec, and at 85 ºC this difference is almost an order of magnitude. Calculation of the absorbtion charge, Q_t, and absorption capacitance, C_t, showed that at -55 ºC and RT, Q_t is in the range from 0.24 C to 0.25 C, and, respectively, C_t is 27% to 28% of the nominal value, C_0. At 85 ºC Q_t increases to 0.44 C and C_t rises to 49% of C_0. These values of C_t are substantially greater than the values observed for capacitors with lower values (12% to 19 %) [3].

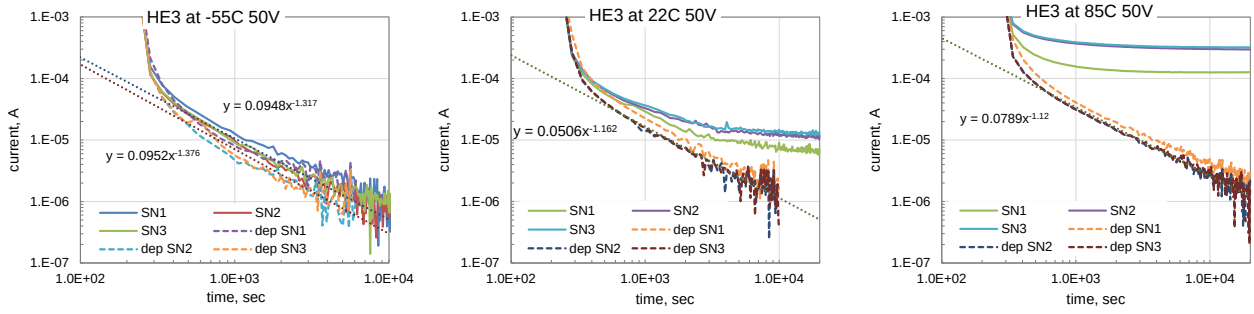

Figure 7. Polarization and depolarization curents in HE3 capacitors at -55 ºC (a), room temperature (b), and 85 ºC (c). Dashed lines correspond to depolarization currents.

Measurements of *I-t* characteristics for HE3 capacitors were carried out consecutively at 5 V, 10 V, 20 V, 30 V, 40 V, and 50 V at temperatures from room to 145 ºC. To present *I-V* characteristics in Schottky coordinates, the thickness of the dielectric was calculated similarly to the THQ3 parts but at VR = 50 V and α_F = 1.5. Calculations yielded *d* = 130 nm.

Current-electric field characteristics at different temperatures in Schottky coordinates are shown in Fig. 8a. The slopes of the lines varied from 2.1E-4 $(m/V)^{0.5}$ at RT to 1.2E-4 $(m/V)^{0.5}$ at 145 ºC. The theoretical value at the high frequency dielectric constant, ε = 5, and RT is 6.5E-4 $(m/V)^{0.5}$ and 4.6E-4 $(m/V)^{0.5}$ at 125 ºC (at ε = 10 these values are 4.7E-4 and 3.5E-4 $(m/V)^{0.5}$). Although the linearity of *I-E* characteristics in Schottky coordinates and decreasing of the slope with temperature are consistent with the Schottky model, the values of the slope are more than three times lower than the theoretical values. This might be due to inaccuracy of dielectric thickness assessments, variations of high-frequency dielectric constant, and effect of absorption currents that are difficult to avoid completely.

Temperature dependencies of leakage currents at different voltages are shown in Fig.8b and indicate activation energies ~ 0.4 eV. This value is lower than what is typically observed for wet tantalum capacitors, 0.75 ±0.1 eV [3] and might be due to specifics of electrolyte used in these parts or to a relatively thin dielectric. The latter factor increases electric field in the oxide and reduces the Schottky barrier.

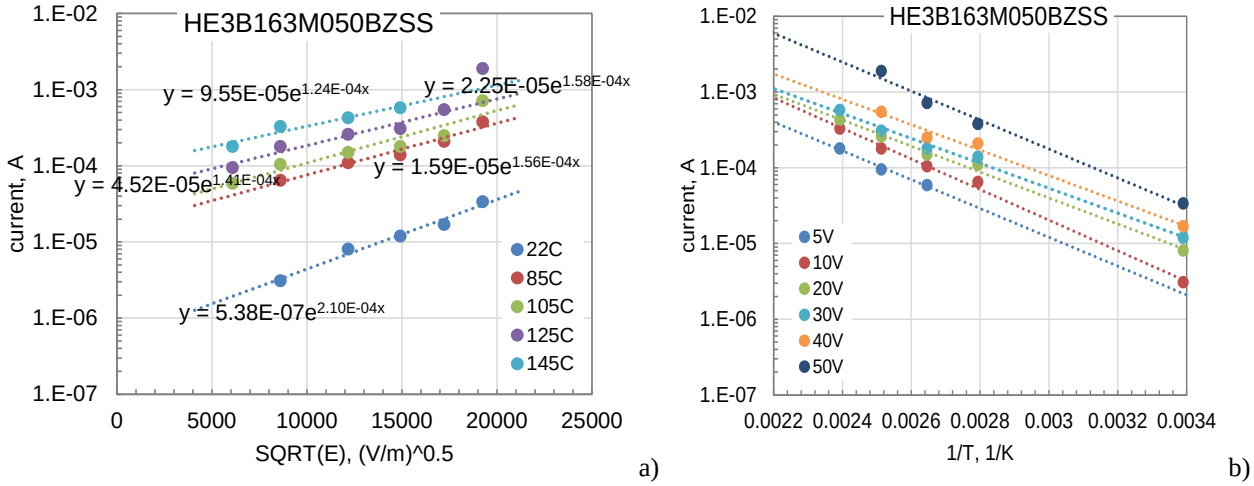

Figure 8. Variations of leakage currents with electric field (a) and temperature (b) for HE3 capacitors.

Highly accelerated life testing (HALT) was carried out for 100 hours consequently at temperatures 85 ºC, 105 ºC, 125 ºC, 145 ºC, and 160 ºC To avoid overstress of the parts, the stress voltage for HE3 capacitors was reduced to 40 V and to 60 V for THQ3 capacitors. Due to high level of currents at 160 ºC, the power supply voltage dropped and was below the set voltage. After HALT, the parts were baked at 150 ºC for 100 hours.

Results of testing at 105 ºC, 125 ºC, and 145 ºC are shown in Fig.9. In all cases, after initial relaxation due to absorption processes, currents are increasing with time, reaching maximum, and then decreasing again. For HE3 capacitors, the time to maximum is decreasing from more than 100 hours at 105 ºC to ~35 hours at 125 ºC and to ~ 20 hours at 145 ºC. Interestingly enough, similar times to maximum were observed for THQ3 capacitors.

A similar behavior of leakage currents with time was observed during oxidation of tantalum sheets in nitric acids at constant voltages by Vermilyea (1955), Jackson (1973) [6], and Hossick-Schott (2009) [7]. The presence of maximum was explained by field-induced crystallization. Time to the current minimum corresponds to the incubation period after which the crystalline oxide starts growing, breaks amorphous oxide and causes increasing currents. The following formation of the crystalline oxide results in decreasing currents with time.

It is also possible that increasing leakage currents are due to migration of positively charged oxygen vacancies that result in reduction of the barrier at the electrolyte/Ta2O5 interface. The effective activation energy of the time to maximum is in the range from 0.7 eV to 0.9 eV, which is close to the activation energies of migration of oxygen vacanies. The following neutralization of the charge by electron trapping results in decreasing currents with time.

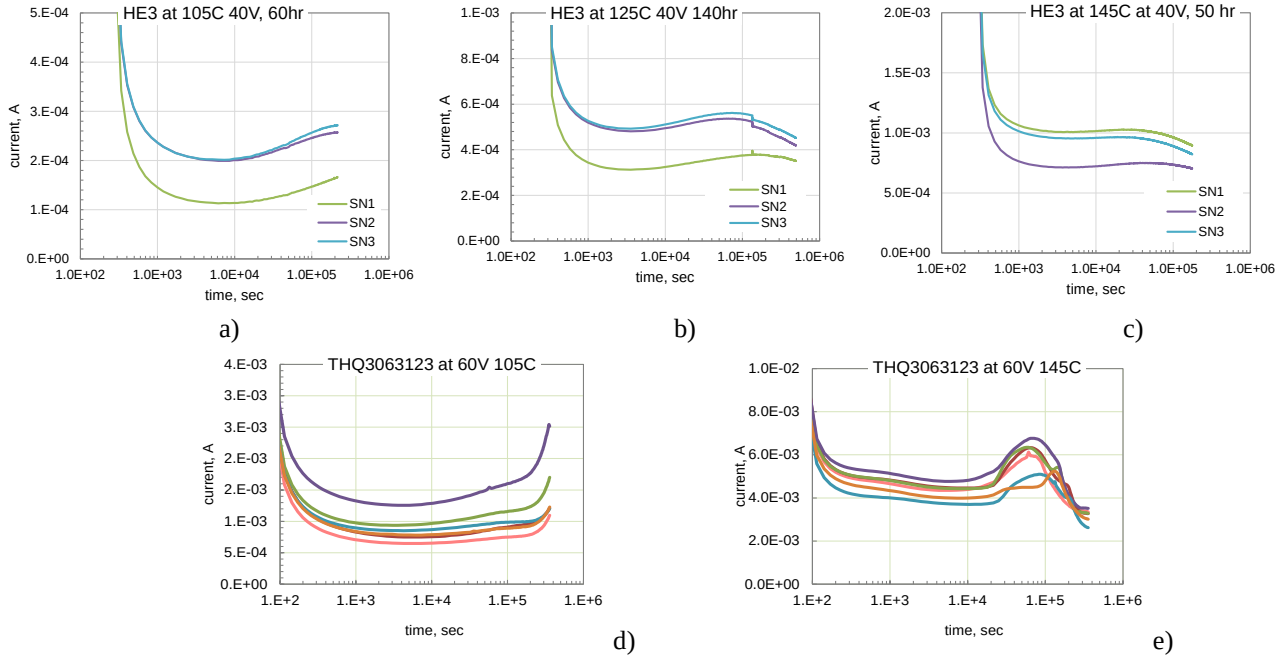

Figure 9. Variations of currents with time during 100-hour testing at different temperatures for HE3 (a – c) and THQ3 (d, e) capacitors.

Post-HALT measurements at room temperature showed anomalies in current relaxation in two out of three tested HE3 capacitors (see Fig. 10) and in 2 out of 6 THQ3 capacitors (see Fig. 11). One of HE3 capacitors, SN2, had increased currents after HALT at 145 ºC and the same sample showed anomalous relaxation after HALT at 160 ºC. After bake at 150 ºC one more sample, SN1, had currents substantially, approximately an order of magnitude, greater than normal. Note that after HALT the currents remained within the specified requirements, and failed marginally only after the bake. Depolarization currents in all three capacitors were identical, and no significant variations in leakage currents after HALT was detected for capacitors with normal relaxation (SNs 1 before bake and SN3 after all stresses).

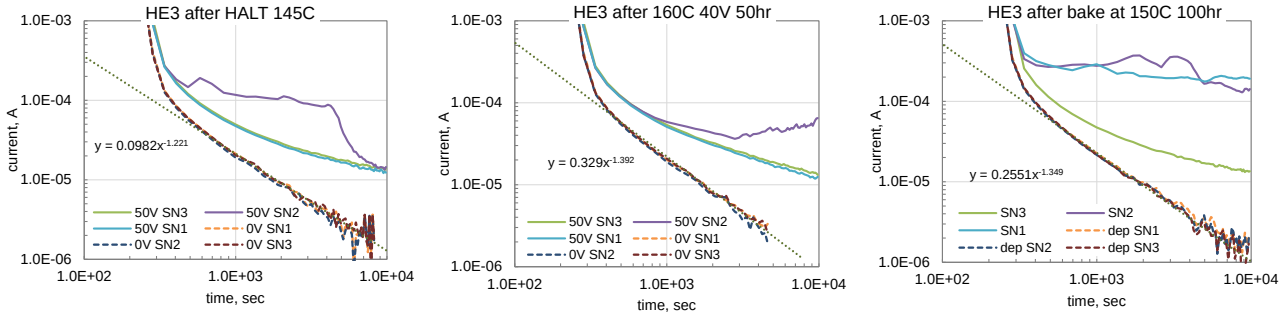

a) b) c)

Figure 10. Relaxation of leakage currents at room temperature in HE3 capacitors after HALT at 145 ºC (a) and 160 ºC (b) and after bake at 150 ºC (c). Dashed lines show depolarization currents.

Anomalies in current relaxation were observed also after HALT at 160 ºC in two THQ3 capacitors (see Fig.11). Leakage currents increased almost two orders of magnitude resulting in parametric failures. Similar anomalies in HE3 and THQ3 capacitors might be attributed to the presence of electrolyte at the glass seal area [3].

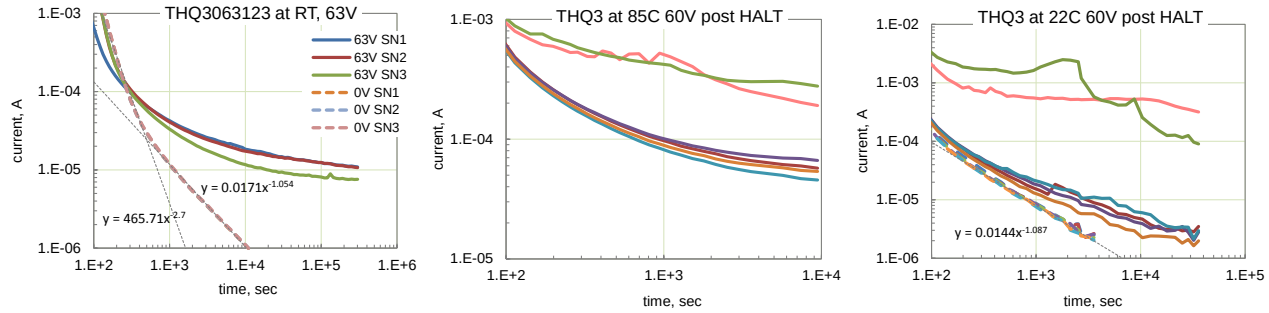

a) b) c)

Figure 11. Relaxation of leakage currents in THQ3 capacitors at room temperature initially (a) and after HALT at 165 ºC 60 V 100 hr (b, c).

External examination of the capacitors after testing showed evidences of electrolyte leak in HE3 samples SN1 and SN2 and in two THQ3 samples with anomalous current relaxation. Images of the leaky parts are shown in Fig. 12. Note that capacitance and dissipation factors remained the same, and no changes between the initial and post_HALT *C-f* characteristics were observed.

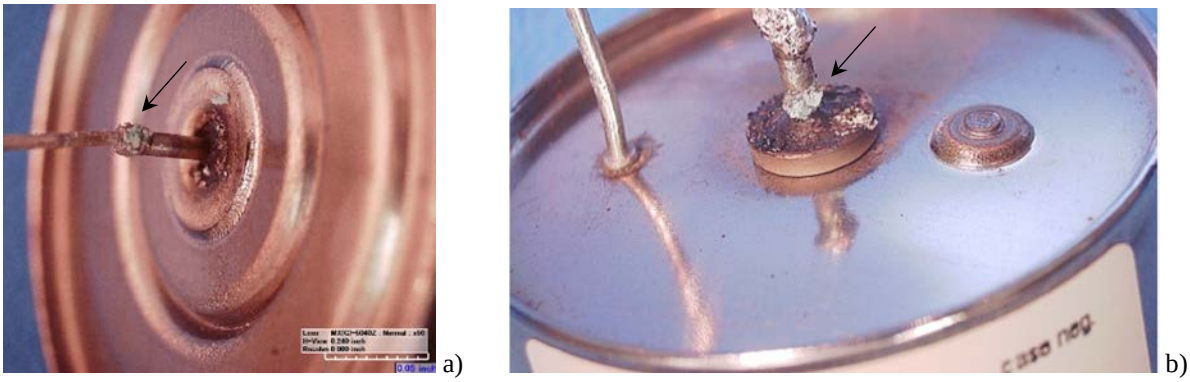

a) b)

Figure 12. External views of the leaky HE3 (a) and THQ3 (b) capacitors. 2/6 HE3 after HALT and100 hr at 150 ºC

After 1.5 months of storage at room conditions, relaxation of leakage currents in HE3 capacitors that had been stressed by HALT was measured again (see Fig. 13a). All parts had leakage currents within the specification limits. Currents in sample SN3 decreased to below 20 μA after 1 hour of polarization, whereas two other capacitors with evidences of leak at the weld had increased leakage currents after 5 min of electrification. Sample SN3 was used for displacement testing described in the next section, and monitoring of leakage currents continued for samples SN1, SN2 and SN4 that appeared normal after 100 monitored temperature cycles between room temperature and 125 ºC (see Fig 13b). Anomalies in behavior of leakage currents in SN1 and SN2 became more obvious with time of testing. Both samples had unstable currents that reached maximum after a few dozens of hours of testing. Visual examination of the parts during the testing revealed a substantial increase of the volume of the dried electrolyte at the weld area in SN1 and SN2. Figure 13c shows a large amount of blue material (dried electrolyte) at the tube weld in SN2 (compare this picture with Fig.12a where only a small amount of the material at the weld was detected after HALT). Apparently, gas generation increased pressure in the case and forced electrolyte leakage through the compromised weld.

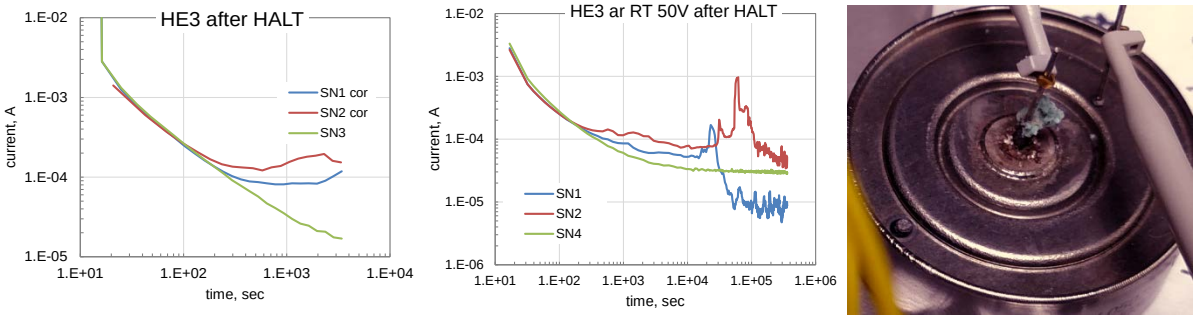

Figure 13. Relaxation of leakage currents in HE3 capacitors after HALT and 1.5 month of storage at room conditions (a) and during 100 hour testing at RT and 50V (b). Fig. (c) shows a view of SN2 after 70 hours of testing.

Results show that a leak of electrolyte can occur in parts with electrical characteristics within the specified limits. Anomalies of leakage current behavior might be used as indicators of the compromised seals. This requires monitoring of leakage currents during screening and qualification testing.

Displacement test

Displacements of the lid in the button case capacitors was carried out using a laser-optical displacement measuring system, ILD1700-40, manufactured by Micro – Epsilon. The laser beam was focused on the central area of the lid close to the glass seal (see Fig. 14). Flexible Minco heaters and a thermocouple were attached to the cylindrical surface of the part and isolated with Teflon tape. Leakage currents were monitored by measuring voltages across a 100 ohm resistor connected in series with the part. A set-up consisted of two power supplies, one to bias the capacitor and another for the heaters, and a data logger. Power supplies were controlled by a PC and the data logger measured temperature, displacement, power supply voltages, and leakage currents. Calibration showed that the sensitivity of displacement measurements was 0.244 mV/μm.

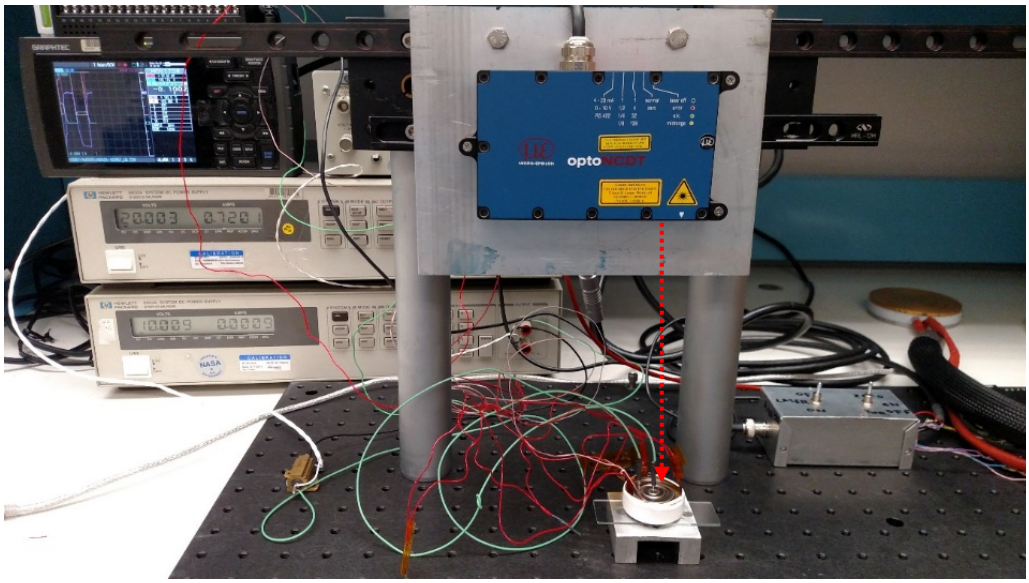

Figure 14. Overall view of the set-up for displacement measurements. Dashed red line indicate location of the beam.

The first test had a purpose of evaluating the effect of multiple current transients on gas generation and deformation of the case. An HE3 sample, SN6, was monitored every 10 seconds during 1650 ON/OFF cycles. The duration of one cycle was 100 sec, 50 sec at 50 V and 50 sec at 0V as shown in Fig. 15 (a) and (b). The heaters were not used for this testing. During the transients, currents exceeded 10 mA for at least 5 seconds and were greater than 0.5 mA for up to 50 seconds under bias. Note that the characteristic time of the RC circuit was 1.6 sec, so the current during first 5 sec was mostly due to the charging and discharging processes. However, charging currents should decrease to below 2 μA after 20 sec, whereas actual currents were above 0.5 mA (see Fig. 15b). These currents were decreasing with time and were due to absirption processes in the dielectric.

No systematic increase in the displacement that would be expected in case of gas generation as a result of transients was observed (see Fig. 15c). However, there was a clear correlation between the displacement and temperature variations in the room. Variations of temperature ~ 0.5 ºC resulted in the lid displacement of ~ 2 μm.

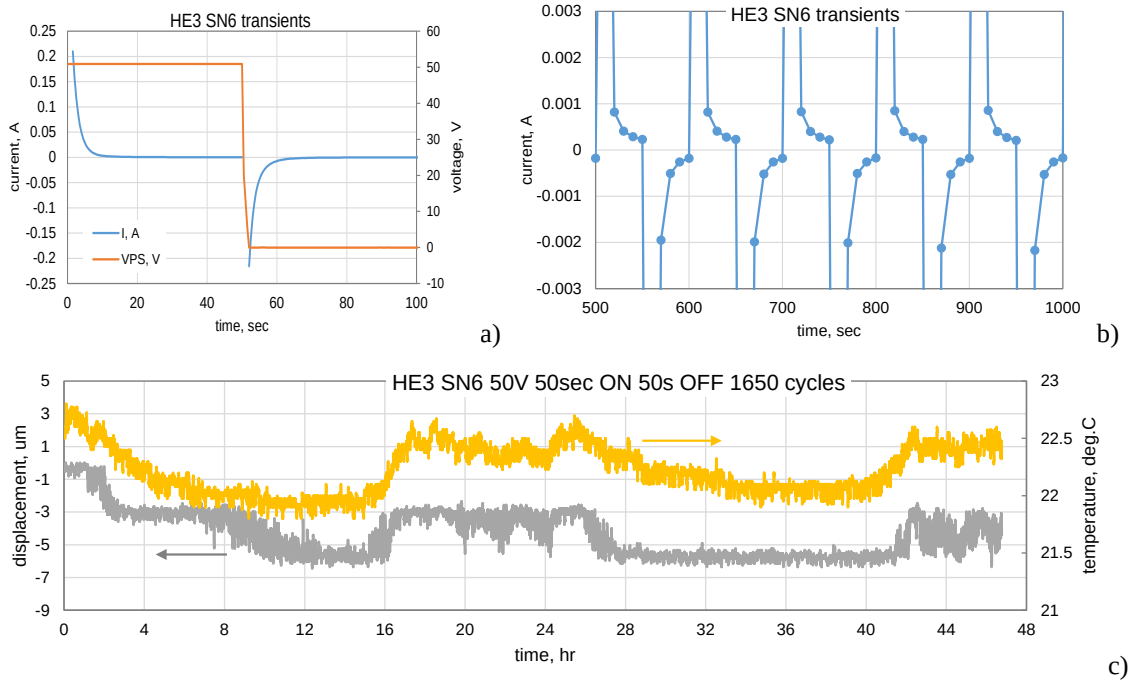

Figure 15. Current transients during 50 sec ON/50 sec OFF cycling in HE3 capacitors during one cycle (a), during several cycles (b), and variations of the displacement and temperature during 1650 cycles (c).

After the testing, sample SN6 was stressed by reverse bias that is known to create substantial case deformation in wet tantalum capacitors [8]. First, the power supply was set to 0.5 V reverse bias for 65 hours. This resulted in currents increasing from ~ 0.3 mA to ~3.5 mA (see Fig.16a), so the actual voltage drop across the capacitor was changing from 0.3 V initially to ~ 0.15 V by the end of this period. No substantial displacement was detected during this testing. The power supply voltage was increased to 1 V for 5 hours. The leakage current increased to ~ 8 mA, and again, no deflection of the lid was detected.

For the next testing the voltage was increased to 1.25 V, which resulted in currents averaging at ~ 9 mA (see Fig.16b), so the actual voltage drop across the capacitor was ~ 0.3 V. No substantial displacement was detected during 21 hours of testing.

To further increase reverse currents, a 100 ohm current sensing resistor was replaced with a 10 ohm resistor. Testing with Power Supply (PS) set to 3 V for 20.5 hours also did not result in any significant deformation of the case. The voltage drop across the capacitor during this testing stabilized at 0.5 V and the reverse current was ~250 mA.

After that, the current sense resistor was reduced to 1 ohm. Results of this testing are shown in Fig. 16 c, d. The reverse voltage across the capacitor increased instantly to ~ 0.75 V and the current to ~ 2 A (maximum PS current). Case temperature raised above the environmental temperature of 22 ºC by ~3 ºC in approximately one hour, and then increased gradually up to ~ 30 ºC after 7 hours of testing. After 27 hours, the current started decreasing and voltage across the capacitor increasing. The process lasted approximately 1.5 hour, during which deformation increased substantially at a rate ~50 μm/min. Eventually, deformation exceeded 1 mm and reached the limit of the test set-up, 1.05 mm. Temperature during this period increased to 35 ºC. After 28.4 hours the power supply voltage was switched to 0 V and testing continued for several hours more. The temperature returned to 22 ºC in ~ 30 min, but the displacement remained above 1.05 mm.

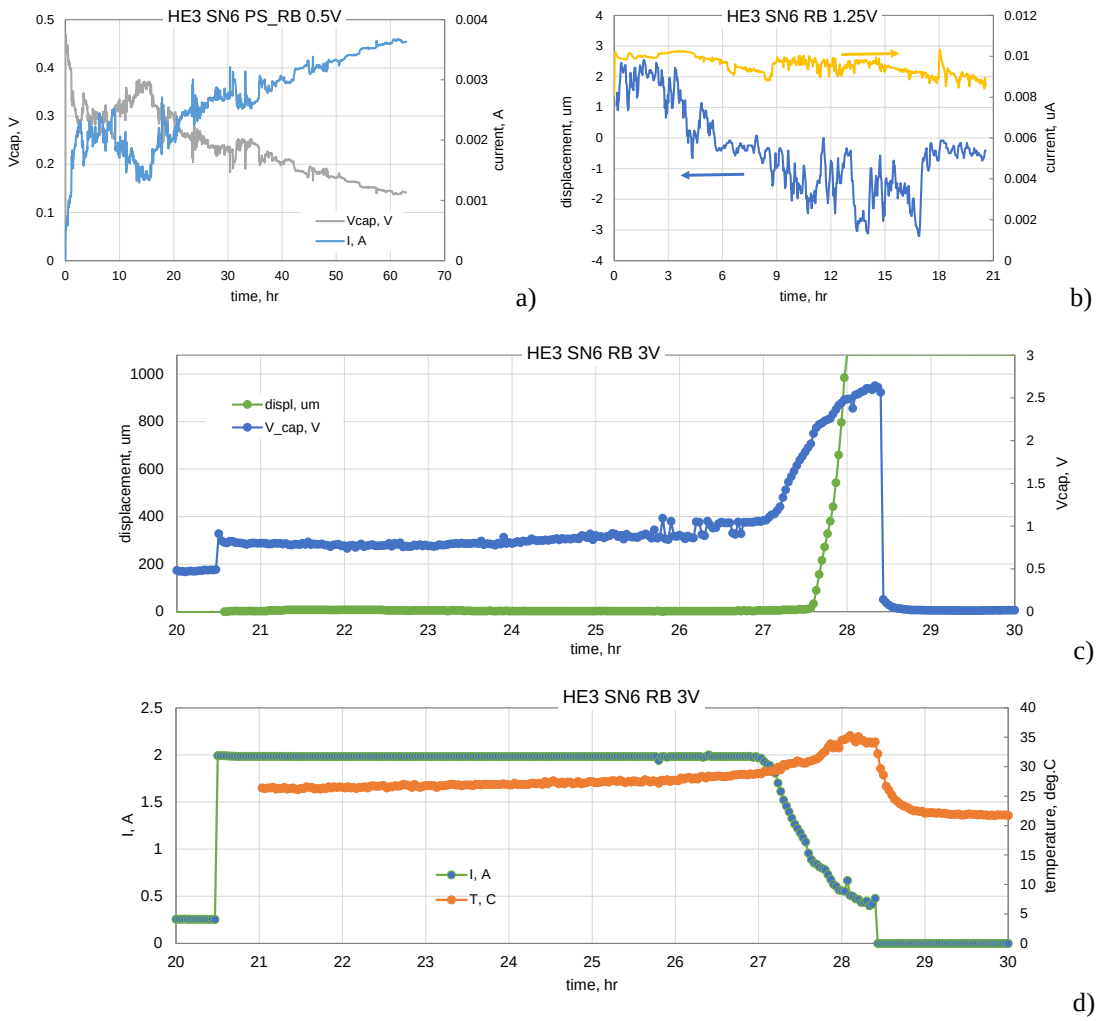

Figure 16. Reverse bias testing of HE3 capacitor SN6 under PS = 0.5 V and R_{sens}= 100 ohm (a), PS = 1.25 V and R_{sens}= 100 ohm (b), and PS = 3 V and R_{sens}= 10 ohm up to 20.5 hours and 1 ohm after 20.5 hr (c, d). The power supply was turned off after 28.4 hours.

A summary of reverse bias testing is shown in Table 1. The table shows also the charge trasnsferred during the testing and calculated as a product of time and average current. Results show that a substantial charge was transferred before the case started bulging.

Table 1. Results of reverse bias testing of sample SN6.

V_PS, V	R_sens, ohm	Duration, hr	V_{cap}, V	I_{cap}, mA	Displacement, um	Charge, C
0.5	100	65	0.3 → 0.15	0.3 → 3.5	< 2	585
1	100	5	0.19 – 0.21	8.3 → 8.1	< 2	144
1.25	100	21	0.3 – 0.4	10 → 8.5	< 2	680.4
3	10	20.5	0.36 → 0.5	260 → 250	< 2	18450
3	1	6.5	0.7 → 1.1	2000	<10	46800
3	1	1	1.07 → 2.57	2000 → 400	> 1050	4000

A substantial bulging of the case after testing could be observed visually, see Fig. 17a. However, the case was not compromised and no electrolyte leak or hermeticity loss was detected. The part was shorted and had a current of > 10 mA at 50 V. Frequency dependencies of the part showed a substantial reduction of capacitance and increase in ESR (see Fig. 17 b, c). Internal examinations (Fig.17.d) revealed delamination of the cathode coating from the tantalum plate that explains a substantial decrease in capacitance.

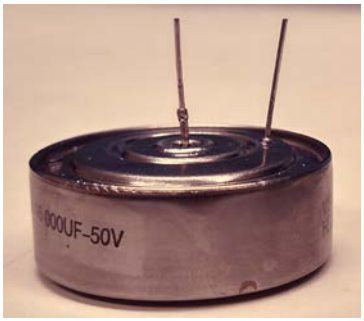

a)

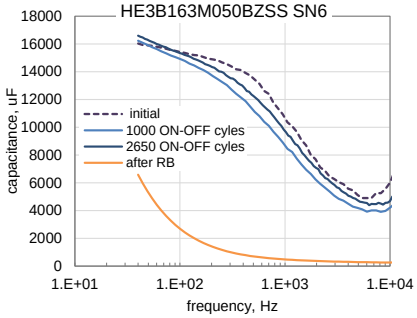

b)

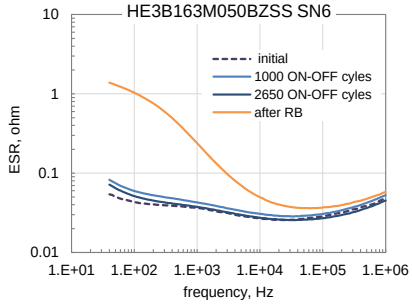

c)

d)

Figure 17. An overall view of SN6 after reverse bias testing showing bulging of the case (a) and frequency dependencies of capacitance (b) and ESR (c). Tantalum cathode plate and polymer separators with remnant of the cathode layer (d).

Displacements in another sample of HE3 capacitors, SN5, were measured during temperature cycling caused by power cycling of the heaters. The amplitude of voltage pulses applied to the heaters increased incrementally to allow temperature stabilization at different levels. Typically, temperature stabilized approximately in 20 min after voltage application. Results of this testing are shown in Fig. 18. Temperature excursions up to 100 ºC resulted in reversible deformation of the case. After exposure to 125 ºC, the displacement reached 700 μm and irreversible deformation of 25 μm was recorded (see Fig. 18b). When temperature exceeded 140 ºC, the displacement exceeded 1 mm and irreversible deformation increased to 450 μm. To assure measurements at high temperatures, the set-up was changed to the maximum value of 2500 μm. This maximum was reached at 180 ºC (see Fig. 18d) and remained stable after the heating power was turned off. Currents through the capacitor during the testing that were measured at 10 V increased up to 0.6 mA. This resulted in 6 mW dissipated power that should not have caused any substantial additional increase in the temperature.

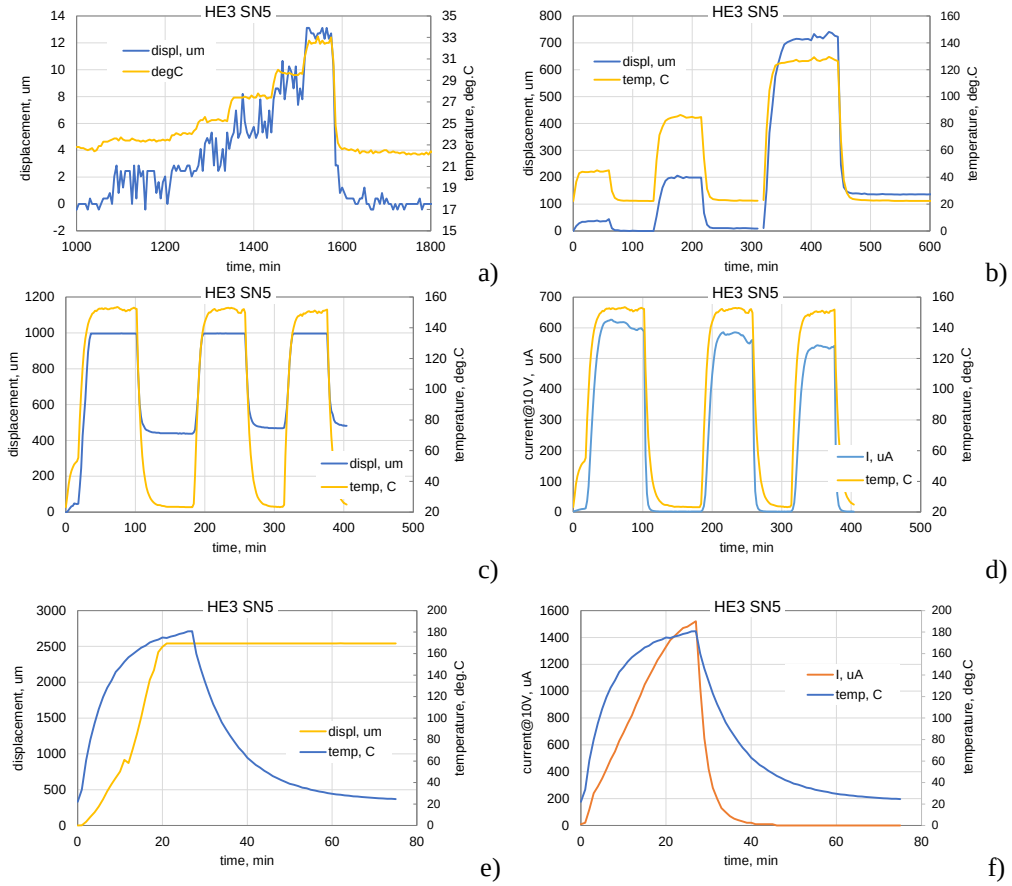

Figure 18. Displacements in HE3 SN5 during temperature cycling.

Based on test results, variations of the displacement with temperature are plotted on Fig. 19. Temperature rise increased displacement exponentially up to 2.5 mm at ~175 ºC.

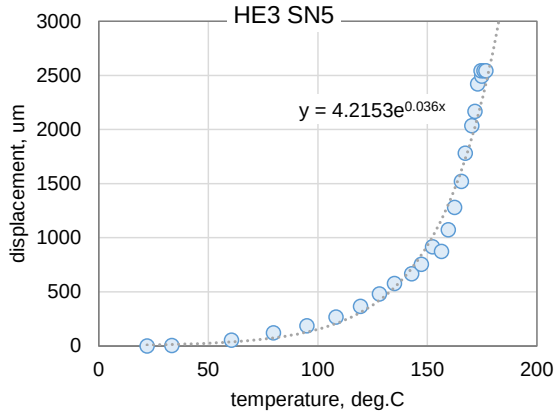

Figure 19. Variation of displacement with temperature for SN5.

An HE3 sample SN4 was first stressed by three low-power heating cyles that resulted in temperature increase to 32 ºC, 43 ºC, and 55 ºC and displacement to 12, 34, and 70 μm (see Fig. 20a). Each cycle consisted of 1 hour power ON and one hour power OFF periods. Next three cycles (see Fig. 20b) increased temperature to 70 ºC, 85 ºC, and 101 ºC and respectively the displacement to 104 μm, 180 μm, and 315 μm.

After that, the part was stressed by 100 cycles (40 min ON and 40 min OFF) that resulted in temperature increase to 125 ºC and displacement to ~ 650 μm (see Fig. 20c). No substantial changes in the amplitude of displacement during this testing was observed. Deformation was reversible during first tests and by the end of testing irreversible deformation reached ~100 μm.

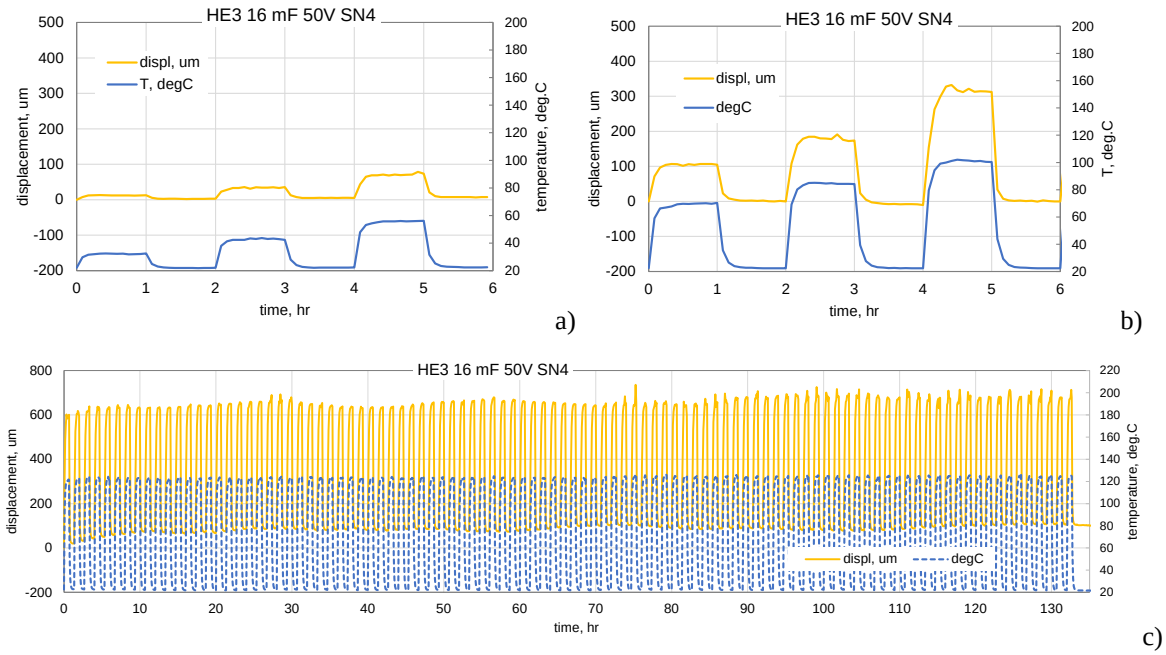

Figure 20. Displacement during power cycling in sample SN4 of HE3 capacitors.

Temperature cycling did not cause any substantial changes in frequency dependencies of capacitance and ESR (see Fig. 21 a, b). However, measurements of leakage currents showed that both polarization and depolarization currents increased (see Fig. 21 c, d). Current readings taken after 1000 sec increased more than two times. Note, that relaxation currents were measured initially using 100 ohm and after cycling using 10 ohm sense resistors. This resulted in different charging/discharging timing and a slower relaxation initially.

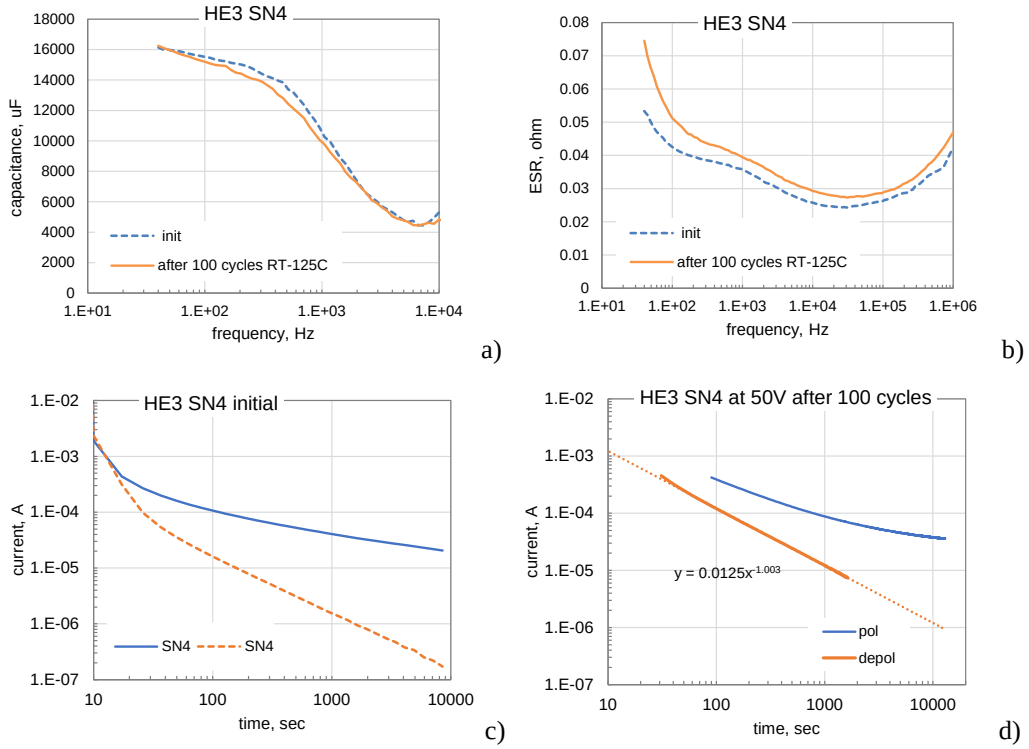

Figure 21. Frequency dependencies of capacitance (a) and ESR (b) and initial (c) and post-cycling relaxations of polarization (50 V) and depolarization (0 V) currents in SN4 HE3 capacitor.

An HE3 sample SN3 that had no case defects and showed normal electrical characteristics after HALT was tested for displacement first with no bias applied and temperature increasing from room to 105 ºC. This resulted in ~90 μm of the case deformation (see Fig.21). After temperature stabilized, a forward bias of 50 V was applied. Currents increased during the first 30 min up to 2.7 mA, and then gradually decreased to ~ 1 mA after 90 hours. Displacement slightly increased during this testing from 185 μm to 203 μm (Fig. 22b).

After testing at 105 ºC, voltage on the heater was increased so the temperature rose to 140 ºC while the part remained at 50 V bias. At 140 ºC the current increased to ~ 8 mA and displacement rose to ~650 μm. After temperature stabilization the displacement continued increasing from ~650 μm to ~900 μm after 4 hours of testing. Continued testing resulted in a displacement spike up to 1300 μm, and electrolyte vapor leaking from the glass seal area was observed. For this reason, testing at 140 ºC was terminated after 5 hours.

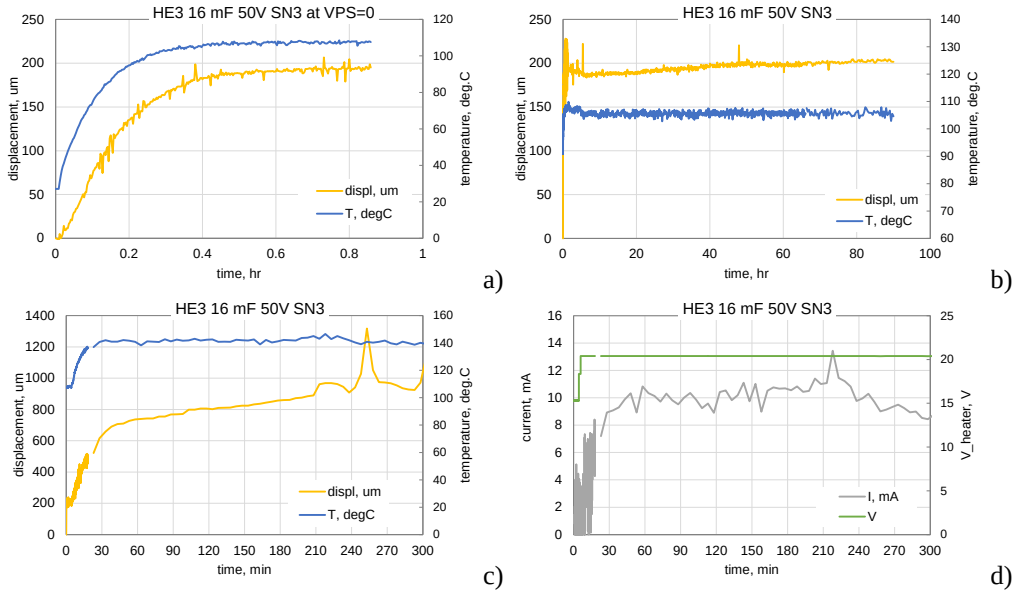

Figure 22. Displacement testing of sample HE3 SN3 at temperatures stabilizing at 105 ºC (a, b) and 140 ºC (c, d).

Visual examinations of sample SN3 showed a large amount of electrolyte and bubbles in the central area of the lid (see Fig. 23a). Optical examinations revealed a crack in the glass (Fig. 23b) that most likely was due to the high internal pressure developed by the generated gas during testing at high temperatures.

Electrolyte leak resulted in a substantial decrease of capacitance, from 15.2 mF initially (at 120 Hz) to 10.4 mF after the testing, and increasing ESR, from 0.0371 ohm to 0.0452 ohm at 1 kHz, (see Fig. 23 c, d). Note that ESR only marginally exceeded the specified limit of 0.045 ohm. Leakage currents measured after 1000 sec of electrification (~ 110 μA) increased compared to the post-HALT results, but still remained below the specified limit.

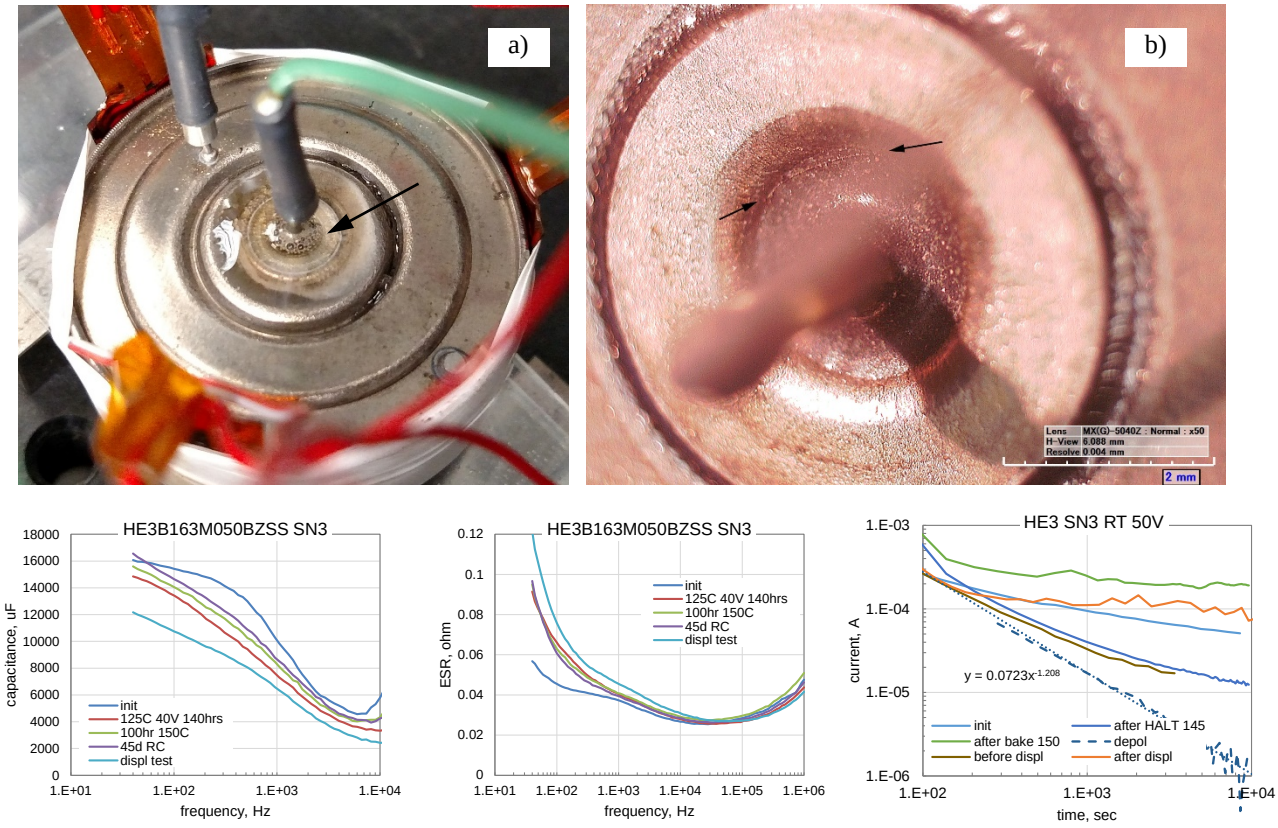

Figure 23. External views (a, b) and electrical characteristics (c, d, e) of capacitor HE3 SN3 after displacement testing. Arrows in Fig. (b) show location of a crack in the glass that resulted in electrolyte leak. Dashed line in Fig (e) corresponds to absorption (depolarization) currents.

Displacements for a sample of THQ3063123 capacitors was first measured at different levels of the power on heaters. Temperature was stabilized at different levels in the range from 33 ºC to 125 ºC and the relevant displacements varied from 7 μm to 330 μm (see Fig. 24).

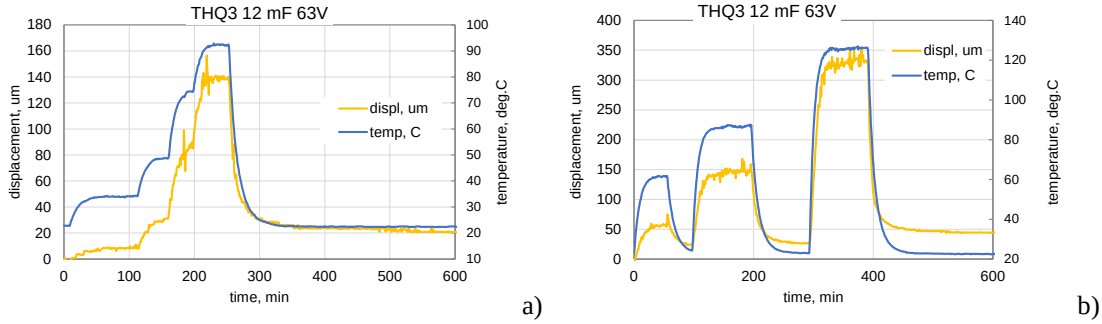

Figure 24. Variation of displacement with time at different levels of the heaters' power for a THQ3 capacitor.

After that the part was stressed at room temperature by 1000 voltage cycles with each cycle having 60 sec at 50 V and 100 sec at 0 V. Similar to HE3 SN6 (Fig. 15) multiple high current transients did not cause substantial variations of the displacement.

The next testing with THQ3 capacitor was carried out during 100 temperature cycles when the heaters were ON for one hour and OFF also for one hour while the voltage across the capacitor was maintained at 30 V. Results of this testing are shown in Fig. 25. Note that the first five cycles were carried out with increasing power of the heater, and the 100 cycle test started after maximum temperature reached 125 ºC. Displacement during this testing changed periodically from 0 to ~ 300 μm and current increased up to 30 μA during the first 125 ºC cycle, but then stabilized at ~ 25 μA.

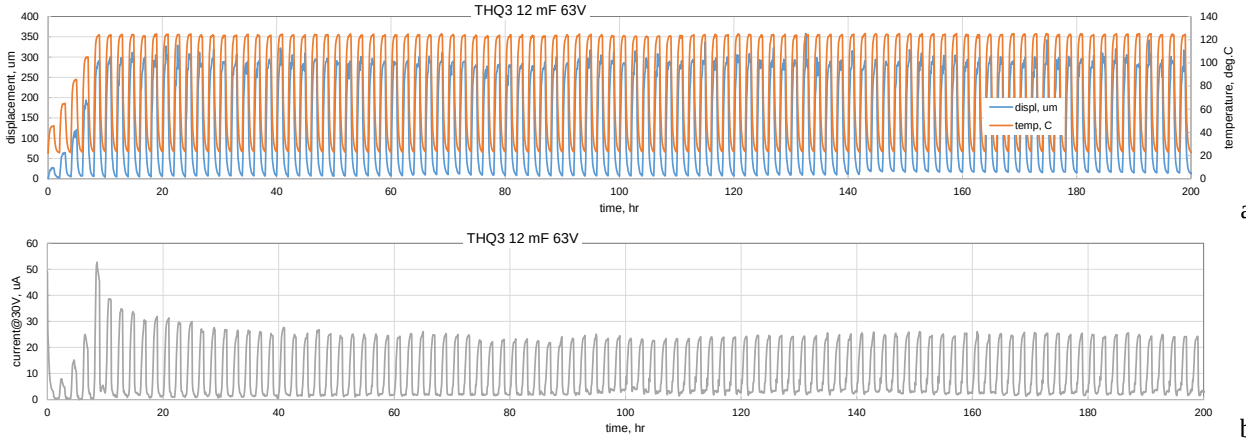

Figure 25. Variations of displacement and temperature (a) and current at 30V (b) during temperature cycling testing of a THQ3063123 capacitor.

Discussion

Results of this study confirm that case deformation might be due to increased vapor pressure at high temperatures and gas generation as a result of electrochemical processes at the electrodes. Deflection of the lid creates a gap between the protective washer or rubber ring and mating part of the lid thus allowing penetration of electrolyte to the glass seal and tubing weld areas. This increases leakage currents, makes them unstable, and compromises the seal by weld corrosion or glass cracking.

The pressure of vapor above the electrolyte (~40% solution of the sulfuric acid in water) in the package of wet tantalum capacitor is exponentially increasing with temperature and can be calculated according to an empirical equation [9]:

$$\log(P_{el}) = A_{el} - \frac{B_{el}}{T}, \qquad (1)$$

where P_{el} is in tor, A_{el} = 8.87 and B_{el} = 2286 are constants; T is the temperature in K.

Variations of the pressure in atm with temperature calculated per Eq.(1) are shown in Fig. 26a. Note that the chart shows an excessive pressure caused by the electrolyte vapor. The total pressure is a sum of the air pressure in the can and the vapor pressure. The air pressure in the can at room temperature is 1 atm and increases linearly with the absolute temperature according to the gas law. In vacuum, the excessive pressure will be 1 atm already at room temperature. According to chart Fig. 26a, the excessive pressure and deformation of the case in space would be equivalent to terrestrial conditions at ~ 105 ºC.

Deformation of the case caused by internal pressure P can be modeled by a clamped circular plate under a uniformly distributed load. Maximum deformation at the center (deflection) of a plate with radius R, and the thickness of the wall h, can be calculated as:

$$\varpi_{\max} = \frac{P \times R^4}{64D} \quad , \tag{2}$$

where D is the toughness of the plate:

$$D = \frac{E \times h^3}{12 \times \left(1 - \mu^2\right)} \quad , \tag{3}$$

where E = 185 GPA is the Young's modulus of tantalum; μ =0.34 is the Poisson's ratio.

Considering that for HE3 and THQ3 capacitors R = 17 mm and h = 0.4 mm, the deflection of the plate can be calculated per Eq. (2) and Eq.(3). Assuming that both plates, at the top and at the bottom of the case are deforming similarly, the deformation of the case is:

$$d_{def} = 2 \times \omega_{max} \tag{4}$$

Assuming that $P = P_{el}$ from Eq.(1), the case deformation increases with temperature exponentially as it is presented in Fig. 26b.

Results of calculations as well as the experimentally measured displacements for different capacitors in this study are plotted in Fig. 26b. Experimental results can be approximated with Arrhenius law:

$$d_{def} = 7 \times 10^7 \exp\left(-4727 \diagup T\right) \quad , \tag{5}$$

where d_{def} is in μm, and T is in K.

Calculated and experimental data are in a qualitative agreement. However, the calculated values are 50% to 2 times greater than the experimental data. A better agreement is observed at relatively low temperatures. The discrepancy might be due to several reasons. First, deformation of a clamped circular plate is not equivalent to a lid in a cylinder case that experienced also radial pressure, and second, the anode riser wire connects tubing with the slug thus limiting deformation of the lid. Also, the lid was initially pressed against the rubber ring to protect the glass seal area. This reduces deformation of the lid compared to the unpressed plate. Nevertheless, the model can be used for rough assessments of the case deformation and evaluation of conditions at which the internal seal is compromised and the risks of weld corrosion are increasing.

Increasing temperature to 150 ºC would increase air pressure to 1.43 atm, whereas the vapor pressure would increase to 3.84 atm. At the internal pressure of 5.27 atm and external pressure of 1 atm, the lid deflection should be ~870 μm. Similar estimations at 85 ºC result in excessive pressure of 0.61 atm and deflection ~180 μm.

Excessive pressure in the case operating in vacuum at temperature T can be calculated as

$$\Delta P_{vac} = P_{el} + P_0 \times \frac{T}{T_0} \quad , \tag{6}$$

where P_0 and T_0 are atmospheric pressure and room temperature.

Excessive pressure in air is $\Delta P_{air} = \Delta P_{vac} - P_0$. Temperature variations of ΔP_{air} and ΔP_{vac} are shown in Fig.26c. According to this chart, the excessive pressure in vacuum at 85 ºC would be equivalent to excessive pressure in air at 117 ºC. In this regard, storing or operating in vacuum at 125 ºC would be equivalent to storing or operating in air at 140 ºC. Assuming a 10 ºC margin, to assure that the part can operate in vacuum at 125 ºC, high temperature storage (HTS) testing at 150 ºC for 1000 hours is recommended. If maximum operating temperature can be reduced to 85 ºC, the HTS testing can be carried out at 125 ºC.

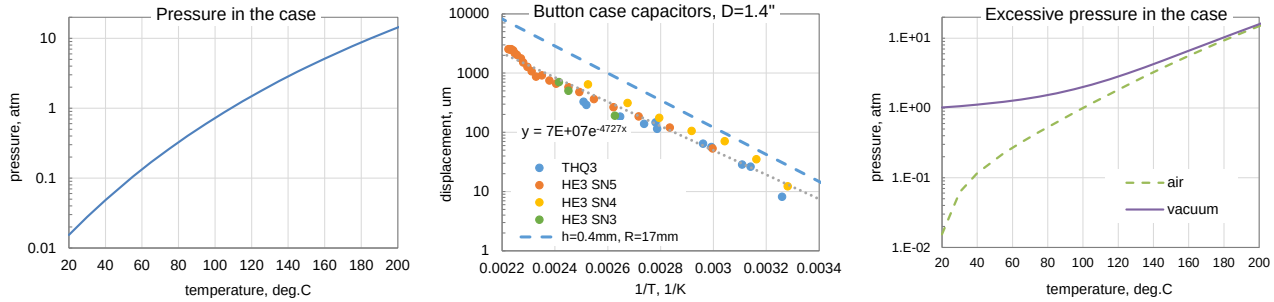

a) b) c)

Figure 26. Variations of the internal case pressure (a), case displacement (b) and excessive pressure (c) with temperature. Dashed line in (b) indicates calculations based on Eq.(4).

Estimations of the gas pressure generated with time by current flowing through a capacitor can be done by assuming that cathode reaction results in generation of hydrogen [3]. According to Faraday's law, the mass of hydrogen, *m*, is proportional to the transferred charge, *Q*:

$$m = \frac{M}{z \times F} \times Q \quad , \tag{7}$$

where, M = 2 g/mol is the molar mass of hydrogen, z = 2 is the number of moles of electrons needed to form one mole of H_2, and F = 96,485 C/mol is the Faraday constant. In this case,

$$n_m = \frac{m}{M} = 5 \times 10^{-6} \times Q \, , \tag{8}$$

where Q is in Coulombs and $n_m = m/M$ is the amount of moles of generated H_2.

Assuming that all generated hydrogen remains in the case of a volume V, the gas pressure, P, can be calculated using the gas law:

$$P = n_m \times \frac{RT}{V} \quad , \tag{9}$$

where R=8.13 J/K is the universal gas constant; T is the absolute temperature.

Considering that the volume of the case is ~ 12 cc and approximately 50% is occupied by porous slugs, washers and separators, a 1 C charge would increase pressure by 5E3 Pa.

Integration of absorption currents during transients in the process of 1650 voltage cycles resulted in more than 42 C of the transferred charge. According to Eq.(8) and Eq.(9), this should have resulted in a pressure ~ 2 atm and deflection ~450 μm. However, no substantial deflection has been observed. Apparently, most of the generated gas was absorbed in tantalum or diffused through the wall or seal of the case [3].

Testing of sample SN3 (see Fig 22) showed that during 90 hr at 105 ºC and forward currents exceeding 1 mA the displacement was ~18 μm. At a transfer charge of 324 C, the deformation should be much greater. Apparently, a substantial portion of the generated hydrogen during this testing was also absorbed by the case. The following testing at 140 ºC for 4 hours increased the current-induced displacement by 250 μm. The charge transferred during this testing was ~260 ºC and the additional pressure should be ~ 13 atm, whereas the deformation corresponded to a pressure of ~ 3.3 atm only. This might be die to a substantial amount of gas escaping the case.

One hundred unpowered cycles between room temperature and 125 ºC that was carried out for sample SN4 resulted in periodical displacements ~ 650 μm. Deformation during first cycles was reversible, but after ~ 20 cycles a remnant deformation of ~ 100 μm developed and remained stable until the end of testing (see Fig. 20). This testing did not change substantially the frequency dependencies of capacitance and ESR, but increased leakage currents. Polarization and depolarization currents measured after 1000 sec increased more than two times. Relaxation of leakage currents appeared normal, and was different compared to the behavior of parts after HALT that was attributed to the presence of electrolyte at the glass seal area (see Fig. 10, 11). Most likely, the observed results are due to exposure of the part to high temperatures. High temperature storage typically results in increased lekage currents in wet tantalum capacitors (to be published).

According to Table 1, charges of hundreds and thousands of Coulombs have been transferred during reverse bias testing. This should have created high internal gas pressure and resulted in bulging or even rupture of the case. At the voltage drop across the capacitor in the range from 0.7 V to 1.1 V and reverse currents of 2 A, the transferred charge during 6.5 hours was 46,800 C, but the deflection was below 10 μm. A substantial bulging of the case was observed only within an hour of the end of testing when currents decreased to ~ 0.4 A.

Large transfer charges during reverse bias testing that did not result in any substantial gas generation indicate a non-Faradaic charge transfer. This is possible if shorts between the anode slug and cathode plates are formed. Internal examinations and XRF analysis revealed spots of Cu/Pd compositions on the surface of polymer separators (see Fig 17.d). Similar spots were also observed on the surface of the tantalum slugs (see Fig. 26). Most likely, ions of copper and palladium under reverse bias conditions are migrating to the slug and depositing on its surface. Some deposits are also formed on the porous separators thus creating a short and allowing electron transport across the formed metal bridges. Note that at the specific resistivity of palladium of ~1E-7 ohm*m, a tiny wire with a length of 0.1 mm and diameter of 3 μm would resulted in a 1 ohm short.

Additional testing have shown that similar shorts might be formed during several hours of testing at reverse bias voltages as low as 0.5 V. This indicates that special measures should be taken during circuit design and testing to assure that no reverse bias of more than 0.5V is applied to the part for more than a few minutes.

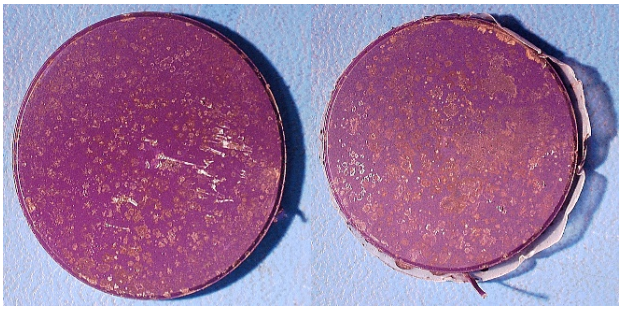

a) Spots on the surfaces of tantalum slugs.

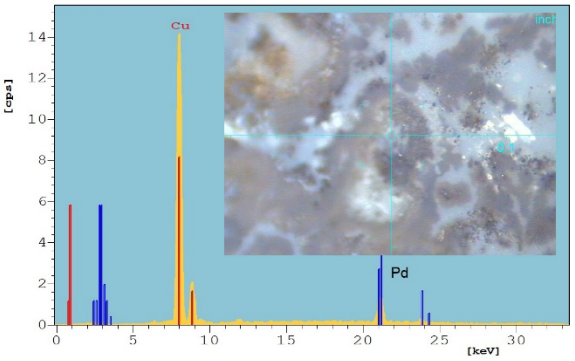

b) XRF spectrum of the dark area on the separator indicating Cu and Pd.

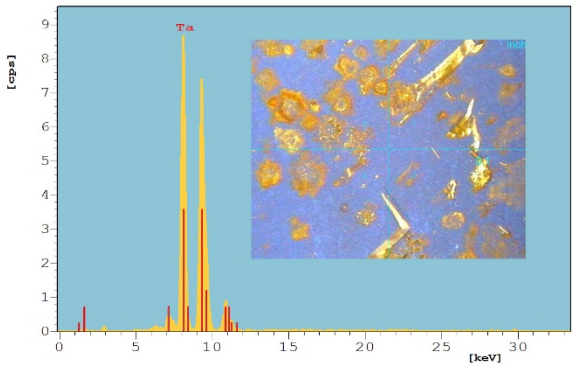

c) XRF of clean area on the slug showing Ta

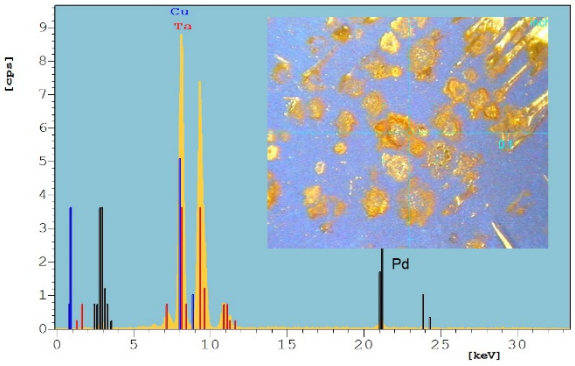

d) XRF of spot area on the slug showing Ta, Cu and Pd.

Figure 26. Optical views of tantalum slugs (a) from SN6 after reverse bias testing and XRF spectrums of the separator (a) and slugs (b, c, d). Inserts on the XRF charts show optical images of the tested areas.

Because some gas generation still occurs even in a capacitor with internal shorts, lid deflection occurs. With time, after 6.5 hours of reverse bias testing, gas generation was apparently sufficient to start bulging the part. As distances between the cathode plate and separator and/or separator and the slug are increasing, the number of shorting contacts reduces. This process goes along with increasing Faradaic portion of the currents and the case continue bulging in spite of reduction of reverse currents.

Sammary

1. Early designs of the button style capacitors had no protection of the glass seal area. This often caused failures due to excessive leak and corrosion of the outlet weld. Introduction of washers between the glass seal and slug/separator reduced the probability of hermeticity failures. However, the effectiveness of this protection is difficult to verify and control. High temperatures and gas generation during operation of the parts can deform the lid and form a gap between the washer and the lid. This might increase leakage currents and the risk of hermeticity leak failures substantially. High temperature storage (HTS) testing is recommended to assure adequate integrity of the parts after possible bulging of the case.

2. Excessive leakage currents result in gas generation and bulging of the case that facilitates electrolyte penetration to the glass seal area. Analysis of leakage currents in HE3 and THQ3 showed the following:
   a. Maximum leakage currents for high-value capacitors are specified at room temperature only, and the requirements are affected by marketing considerations. This reduces the efficiency of the pass/fail DCL measurements for quality assurance purposes. Maximum leakage current at 85 C should be specified based on statistical analysis of experimental results.
   b. Leakage currents in both tested part types were within the specified limits; however, reproducibility and stability of currents was better for HE3 capacitors. During long-term operations (hundreds of hours), the currents have a trend of decreasing with time.
   c. Temperature and voltage variations of leakage currents are consistent with the Schottky model. The intrinsic leakage currents are limited by a barrier at the electrolyte/Ta2O5 interface. Activation energies of leakage currents are 0.4 eV for HE3 and 0.65 eV for THQ3 capacitors.
   d. Increased leakage currents and anomalies in their relaxation after HALT are due to penetration of the electrolyte into the anode feedthrough area. These parts had also hermeticity leaks in the tubing weld.
   e. With proper protection of the glass seal area, HE3 and THQ3 capacitors remained stable even after harsh HALT conditions (145 ºC at rated voltage).
3. A leak of electrolyte can occur in parts with acceptable electrical characteristics. However, anomalies of leakage current behavior might be used as indicators of compromised seals and precursors of future leak failures. To reveal these anomalies, monitoring of leakage currents during screening and qualification testing is recommended.
4. Measurements of the case deformation showed that the lid deflection is exponentially increasing with temperature, see Eq.(5). The deflection is highly temperature sensitive and even small variations of room temperature, from 22 ºC to 22.5 ºC, resulted in ~ 2 μm displacement. Increasing temperature to 125 ºC and to 150 ºC increased the displacement respectively to ~ 600 μm and to ~ 1 mm. At 175 ºC the displacement reached 2.5 mm.
5. One hundred cycles between room temperature and 125 ºC resulted in irreversible deformation of the lid of ~ 100 μm and increased leakage currents approximately two times. Raising temperature to 145 ºC increased irreversible deformation to ~ 450 μm.
6. Calculations of the internal pressure and case deformation based on the transfer charge are substantially less than the experimental values. This is most likely due to hydrogen absorption in tantalum and outdiffusion through the wall and seals of the case.
7. Application of reverse bias to HE3 capacitors of more than 0.5 V even for a few hours can cause short circuit failures due to electrochemical migration of ions of metals that are used in the cathode coating. Additional verification of the system design and application conditions should be made to exclude the possibility of reverse bias during operation and testing.
8. Analysis shows that deformation of the case during operation in vacuum at room temperature is equivalent to the deformation created at normal atmospheric pressure and an ambient temperature ~ 100 ºC. To assure that the part can operate in vacuum at 85 ºC, high temperature storage testing at a temperature of 125 ºC or more is recommended. Requirements for HTS testing will be discussed in the next report..

9. Glass seal protection in button case capacitors is less effective compared to the cylinder case parts. To reduce risks of failures caused by electrolyte penetration to the glass seal and tubing weld areas, a more severe derating is recommended for space applications: maximum case temperature should be limited to 85 ºC. Additional testing is necessary if parts are to be operated at higher temperatures.

Acknowledgment

This work was sponsored by the NASA Electronic Parts and Packaging (NEPP) program. The author is thankful to Michael Sampson, NEPP Program Manager, for support of this investigation, Bruce Meinhold, ASRC Federal Space and Defense, Group Lead, for a review and discussions. Manufacturers' assistance in providing samples for this study and explanations of parts' design and performance are greatly appreciated.

References

1 A. Teverovsky, "Ripple Current Testing and Derating for Wet Tantalum Capacitors," NASA/GSFC, Greenbelt, MD, NEPP Report, 2013, https://nepp.nasa.gov/

2 A.Teverovsky, "Random Vibration Testing of Advanced Wet Tantalum Capacitors," in Quality and Reliability Technical Symposium (QRTS) Hilton Phoenix/Mesa, 2015, p. 2.3, https://nepp.nasa.gov.

3 A. Teverovsky, "Leakage currents and gas generation in advanced wet tantalum capacitors," NASA/GSFC, Greenbelt, MD, NEPP Report, 2015, https://nepp.nasa.gov/.../2015-562-Teverovsky-Final-Paper-NEPPweb-TN2...

4 A. Teverovsky, "Advanced Wet Tantalum Capacitors: Design, Specifications and Performance," in 20th annual International conference "Commecialization of Military and Space Electronics", Los Angeles, CA, 2016, https://nepp.nasa.gov/.

5 D. Evans, "Hermetic hybrid capacitors," 6th International Seminar on Double Layer Capacitors and Similar Energy Storage Devices, December 9, 1996, http://www.evanscap.com/pdf/96-SW.pdf.

6 N. F. Jackson, "Field crystallization of anodic films on tantalum," Journal of Applied Electrochemistry, vol. 3, pp. 91-98, 1973.

7 J. Hossick-Schott, "Charge-based Model for the Time Progression of Field Crystallization in Tantalum Pentoxide," 29th symposium for passive components, CARTS'09, Jacksonville, FL, March 30 - April 2, pp.2.1.1-7, 2009,

8 A. Teverovsky, "Reliability issues with new technology wet tantalum capacitors," in 17th annual International conference "Commecialization of Military and Space Electronics", Los Angeles, CA, 2013, https://nepp.nasa.gov/files/24605/CMSE%202013%20%20WTC%20Teverovsky_n180.pdf.

9 C. H. Greenewalt, "Partial Pressure of Water Out of Aqueous Solutions of Sulfuric Acid," Industrial & Engineering Chemistry, vol. 17, pp. 522-523, 1925/05/01 1925.